Time history effects at the magnetopause: Hysteresis in power input and its implications to substorm processes

M. Palmroth, T. I. Pulkkinen, T. V. Laitinen, H. E. J. Koskinen, and P. Janhunen

Abstract: The energy input processes through the magnetopause are examined in the GUMICS-4 global MHD simulation. We demonstrate that the energy input through magnetopause is strongly controlled by the IMF clock angle, but also on the previous level of magnetic activity. This hysteresis appears in a variety of model runs, and seems to originate from the nature of magnetopause reconnection. These results are shown to imply that the substorm energetics is directly driven by the incoming energy. Based on these results, the differences between the substorm dynamics and substorm energetics are discussed.

Key words: Global MHD simulations, Reconnection, Substorm energy budget.

1. Introduction

The traditional view of the energy input from the solar wind into the magnetosphere is that it is modulated by the solar wind and interplanetary magnetic field (IMF), which control the rate of dayside reconnection [6]. However, a global MHD simulation GUMICS-4 [7] has recently shown indications that the energy transfer through the magnetopause may not only be a function of the present, but also of the past solar wind and IMF conditions [12]. In other words, the energy input through the magnetopause shows hysteretic behavior with respect to the driving solar wind and IMF parameters so that more intense driving implies large energy input even after the driving has already weakened. This result has important implications to the substorm process [13]: The simulation results indicate that if the energy input is evaluated from a quantitative analysis at the magnetopause, energy dissipation in the tail and in the ionosphere are quite directly proportional to it, not showing the characteristic time delays one gets when comparing observational proxies for the driver and the ionospheric dissipation.

In this paper we examine the energy transfer through the magnetopause. Based on series of simulation runs performed using artificial solar wind and IMF driver conditions we discuss the processes at the magnetopause contributing to the hysteresis and the associated time delays. A particular substorm event is used to discuss the implications of the hysteresis on the global energetics and its possible interpretation in substorm processes. In comparisons with observational data, ionospheric dissipation is assumed to be proportional to the AE index [1], while the energy input is parametrized by the often used $\epsilon = (4\pi/\mu_0)vB^2l_0^2\sin^4(\theta/2)$, where μ_0 is the vacuum permeability, v solar wind speed, $l_0 = 7R_E$ a scaling parameter, B

M. Palmroth and H. E. J. Koskinen. Finnish Meteorological Institute, Helsinki, Finland.
T. I. Pulkkinen. Los Alamos National Laboratory, Los Alamos, NM, USA.
T. V. Laitinen and P. Janhunen. Department of Physical Sciences, University of Helsinki, Finland.

the IMF magnitude, and $\theta = \tan^{-1}(B_Y/B_Z)$ the IMF clock angle [2].

2. GUMICS-4 global MHD simulation

The GUMICS-4 global MHD simulation [7] solves the ideal MHD equations in the solar wind and in the magnetosphere, and is coupled to an electrostatic ionosphere at the inner boundary at 3.7 R_E. The upstream boundary conditions (either measured or idealized) are given by solar wind and IMF conditions at the sunward boundary of the simulation. The ionospheric simulation takes the field-aligned currents and electron precipitation at the inner boundary of the simulation mapped along dipole magnetic field lines, and feeds the MHD part with new solution of the electric potential. For more details of the code structure and setup see e.g. [10]. Quantitative methods have been developed to extract the amount of energy entering through the magnetopause surface sunward of $X = -30R_E$ [10], reconnection behavior [9], and energy dissipation in the ionosphere (including contributions from both Joule heating and particle precipitation) [11].

3. Event study

A moderate substorm (AE maximum of about 500 nT) on August 15, 2001, was simulated with GUMICS-4 to examine the energy transfer and dissipation during actually observed solar wind conditions. Fig. 1 shows the observed ϵ parameter giving a proxy for the driver conditions and the AE-index giving a proxy for the ionospheric energy dissipation [1]. Overplotted in a different scale, we show the power transfer through the magnetopause and the ionospheric dissipation evaluated from the simulation. While there is a clear time shift between the observed ϵ and energy input through the simulation magnetopause, the dissipation time sequences have quite similar temporal evolution (with the exception that the simulation does not see the rapid rise in dissipation at substorm onset).

The bottom parts of Fig. 1 show the time differences even more clearly. The four hodograms show the various input and dissipation parameters plotted against each other. It is clear that

using the observational proxies, the system shows increasing input leading to a later dissipation of energy (top left hodogram). The same is true if the ϵ is computed from the simulation at the magnetopause and compared with the dissipation in the simulation ionosphere (top right). However, the plot showing the hodogram between ϵ and the energy input through the magnetopause (bottom left) demonstrates that the time delay associated with the varying solar wind and dissipation in the ionosphere is associated with processes occurring already at the magnetopause; the hodogram between ϵ and magnetopause energy input is identical in shape to those comparing ϵ and ionospheric dissipation. On the contrary, if one examines the energy input through the magnetopause as computed from the simulation and compares that with the energy dissipation in the ionosphere, there is almost no time delay associated with the ionospheric dissipation (bottom right). Hence, the energy transferred through the magnetopause is quite directly processed by the system.
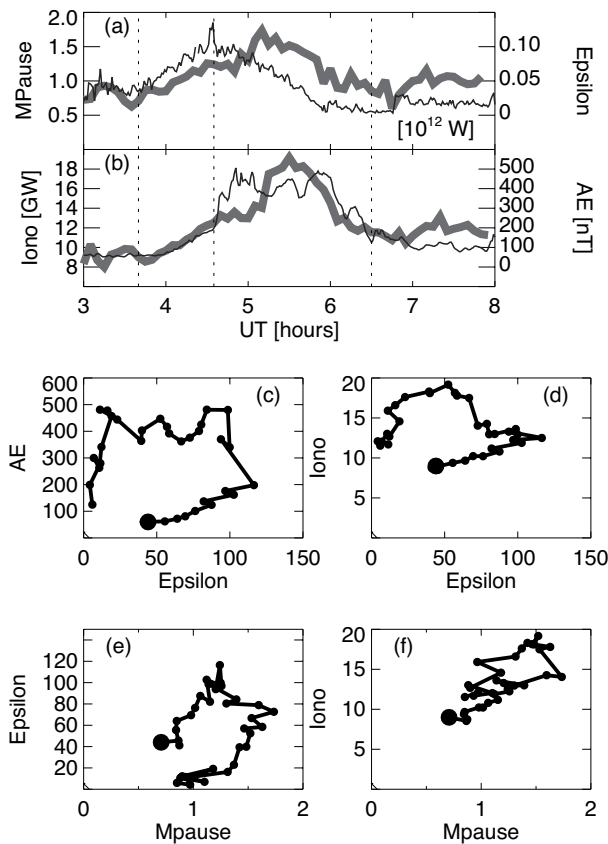
Fig. 1. Substorm on Aug 15, 2001. (a) Energy transfer rate through the magnetopause from GUMICS-4 in 10^{12} W (gray, thick line) and measured ϵ transferred to the magnetopause (black, thin line, scale on the right). (b) Ionospheric dissipation from GUMICS-4 in GW (gray, thick line) and measured AE-index (black, thin line, scale on the right). (c) Hodogram of the observed ϵ vs. AE index. (d) ϵ vs. ionospheric dissipation, (e) magnetopause energy transfer vs. ϵ, and (f) magnetopause energy transfer vs. ionospheric dissipation all from GUMICS-4. The start points are marked by the large filled circle [13].

4. Energy transfer processes at the magnetopause

To systematically investigate the energy transfer at the magnetopause, we ran four simulations with controlled solar wind data. In the four runs, the solar wind dynamic pressure p_{dyn} and magnetic field intensity were kept constant, while the IMF was rotated in the YZ plane from clock angle $\theta = 0°$ to $360°$ with $10°$ steps such that each clock angle value was kept constant for 10 minutes. The full rotation thus lasted for 6 hours. The simulation was initialized by running a steady northward IMF for one hour before the rotation started at the sunward wall of the simulation box. Table 1 summarizes the input parameters.

Fig. 2a-d presents the instantaneous distributions of energy transfer for Run #1, integrated from the nose of the magnetopause to -30 R_E in the tail. Each sector shows the sum of energy transfer taking place in the angular direction shown in the outer circle, viewing from the Sun looking tailward. The IMF clock angle at the time for which the distribution is plotted is indicated with the black arrow. Fig. 2e shows the total integrated energy across the entire magnetopause as a function of the clock angle (solid line). The vertical dashed lines indicate the times for which the instantaneous energy transfer distributions are shown above. The dashed line in Fig. 2e shows the function $\sin^2(\theta/2)$ scaled to same minimum and maximum intensity. We use the second power of $\theta/2$ instead the fourth (which would give a functional form similar to that of the ϵ parameter), as it is a better representative of the simulation results. Thus, the simulation indicates that the energy transfer through the magnetopause scales rather more like the electric field ($\sin^2(\theta/2)$) than ϵ ($\sin^4(\theta/2)$).

The gray area, normalized to 800 GW at the outer circle, and negative values in the line plot indicate energy input from the solar wind into the magnetosphere. For the energy transfer there is no information on the distance at which the energy transfer occurs; however, we have previously shown that the energy transfer occurs predominantly Sunward of the $X = -10R_E$ [10]. The black circles plotted over the energy transfer sectors highlight the locations where reconnection is likely to occur (for a characterization of magnetopause reconnection, see [9]) ranging from the nose of the magnetopause (center of the panel) to the dawn-dusk terminator.

In Fig. 2a, the IMF has rotated for over an hour to $\theta = 60°$. The energy transfer occurs at dawn (dusk) high-latitudes in the northern (southern) hemisphere. Although reconnection does not yet reach the very nose of the magnetopause, it already has a low-latitude component. Hence, the open field lines travel to nightside through dawn (dusk) high latitudes in the northern (southern) hemispheres [4]. As demonstrated in [10], the geometry between the magnetosheath bulk flow and the tailward moving open field line demands that Poynting vector points towards the magnetopause. This implies that electromagnetic energy, which forms the largest component of the transferring energy in all runs at all times, is focused toward the magnetopause at locations where field lines convect to the nightside. This also explains why the energy is mainly transferred sunward of X = -10 R_E [10]: Tailward of that distance the field lines are already more aligned with the magnetosheath bulk flow, making the Poynting vector component perpendicular to the magnetopause small.

In Fig. 2b the energy is still being transferred in the dawn (dusk) sectors in the northern (southern) high latitudes, perpendicular to the reconnection line. As the low latitude reconnection has now fully started, the high latitude convection and consequently the amount of energy over dawn (dusk) sectors in the northern (southern) hemisphere has been enhanced. In Fig. 2c, the clock angle has rotated to $240°$. During the negative IMF y component, the open field lines convect through the dusk (dawn) sector on the northern (southern) hemisphere [4], which is also where the largest energy transfer is taking place, again due to Poynting flux focussing.

Curiously, in Fig. 2c, the dawn (dusk) high latitude sectors in the northern (southern) hemisphere show more enhanced energy transfer than dusk (dawn) sectors in Fig. 2b, although the driving conditions in the solar wind and IMF are identical during these two time instants (except for the sign reversal of IMF y component). Furthermore, the reconnection line is more aligned to low latitudes than in Fig. 2b. Both facts imply that (1) convection has not altogether ceased from dawn (dusk) sectors in the northern (southern) hemisphere, and that (2) there is stronger convection taking place in dusk (dawn) high latitudes in Fig. 2c than in Fig. 2b. Consequently, more energy is being transferred during $\theta = 240°$ than during $\theta = 120°$, which shows also in Fig. 2e. As speculated in [12], this may be due to hysteretic behavior of magnetopause reconnection.

In Fig. 2d, the energy transfer is still larger than during $\theta = 60°$ (Fig. 2a), although the driving conditions during these two time instants are similar (except for the sign reversal of IMF y component). The larger energy input in Fig. 2d is due to more enhanced convection in the primary energy transfer sectors perpendicular to the reconnection line. The more enhanced convection in these sectors may be explained by the orientation of the reconnection line, which is located at slightly lower latitudes (about from $320°$ to $140°$, whereas in Fig. 2a it is aligned from $30°$ to $210°$). Furthermore, the low latitude reconnection has not ceased and the reconnection is still taking place at the nose of the magnetopause (unlike in Fig. 2a). Hence, the comparison of Figs. 2a and 2d suggests that the reconnection line rotation follows the IMF rotation with a delay, explaining the larger energy input in Fig. 2d.

The time delay between the scaled $\sin^2(\theta/2)$ and the total energy transfer is 30 minutes after the due southward IMF in Fig. 2e. For other runs specified in Table 1 the temporal evolution of the total energy transfer is similar as in Fig. 2e [12]. However, the time lag, computed by finding the best correlation for the energy transfer with the $\sin^2(\theta/2)$ after due south IMF, is different in the other runs (Table 1): For larger IMF the time lag increases, while for larger pressures the time lag decreases. The IMF dependence of the time lags support the hypothesis that reconnection processes may be involved in the hysteretic behavior of energy transfer. The pressure dependence may be caused by the smaller size of the magnetopause when the pressure is large that reduces time scales associated with propagation through the system.

5. Summary and discussion

In this paper, we have presented evidence that in GUMICS-4 global MHD simulation the energy transfer through the magnetopause does not directly follow the solar wind driver. Based

Table 1. Synthetic run parameters.

Run #	|IMF| [nT]	p_{dyn} [nPa]	time lag [min]
1	5	2	30
2	10	2	40
3	5	8	20
4	10	8	30

on the simulation results, it appears that after the reconnection has fully begun, it remains active although the driver conditions in the solar wind subside. This is observed in the following aspects in the simulation results:
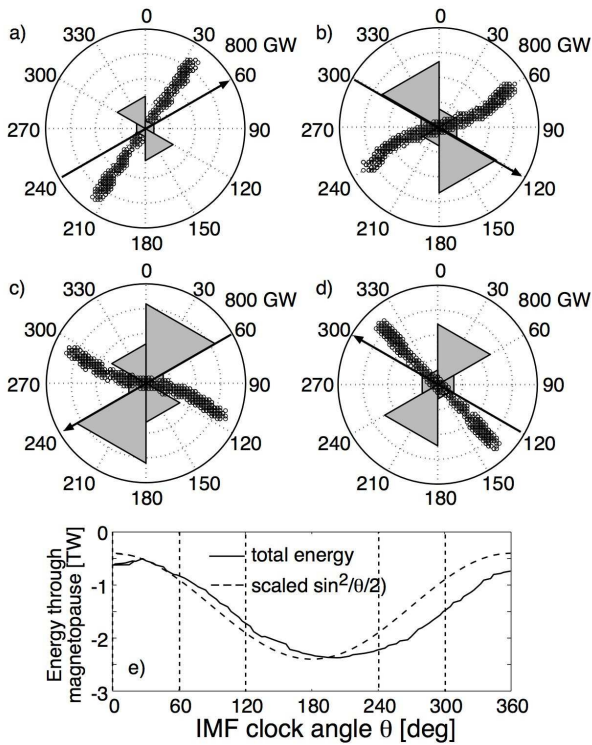
(1) The reconnection line reaches over the subsolar position after due south IMF, although before the due south the line is discontinuous over the subsolar position (compare Figs. 2a and 2d);

(2) The reconnection line follows the IMF rotation with a delay, and thus stays more aligned to low latitudes after due south IMF (compare Figs. 2a and 2d, 2b and 2c); and

(3) The tailward convecting field lines remain open until the tail reconnection closes them, and during the convection the Poynting flux continues to focus toward the magnetopause (compare Figs. 2b and 2c).

These observations from the simulations suggest that the magnetopause reconnection is not only a function of the solar wind driver, but also depends on whether reconnection has previously been active.

In order to test these results, a series of other test runs were performed. The results (not shown) indicate that the hysteresis is a general property of the simulation, not dependent on the run or driver details: The dawn-dusk asymmetry effects of the corotation electric field and Hall conductivity in the ionosphere were tested by a run where the IMF rotation occurred in a counter-clockwise direction. The results were identical to those with clockwise rotation. Possible asymmetry effects related to rotation of the clock angle rather than changing IMF z component was tested by rotating the IMF back from due southward through positive B_y (clockwise rotation from 0 to $180°$ and counter-clockwise rotation from 180 to $0°$). Again, the hysteretic behavior was observed, but this time with a shorter time delay. The speed of the IMF rotation does not eradicate the hysteresis: runs with twice as fast and twice as slow rotation also show hysteretic behavior, but again with a different time delay. An interesting question is what happens if the IMF is rotated clockwise a second time: In this case, after IMF being northward, the energy input followed the IMF rotation as the clock angle increased, identically to what was found during the first rotation. After due southward IMF, the energy input again showed hysteretic behavior with a time delay similar to that in the first rotation. Thus, the northward IMF situation erases the magnetopause memory of past driving.

The ϵ parameter is frequently used to parametrize energy transfer processes at the magnetopause. Our simulation results indicate that

(1) The ϵ parameter does not accurately account for the energy input after the IMF has been negative, i.e., after periods of strong driving. During such conditions, the reconnection line remains at low latitudes and energy input remains large;
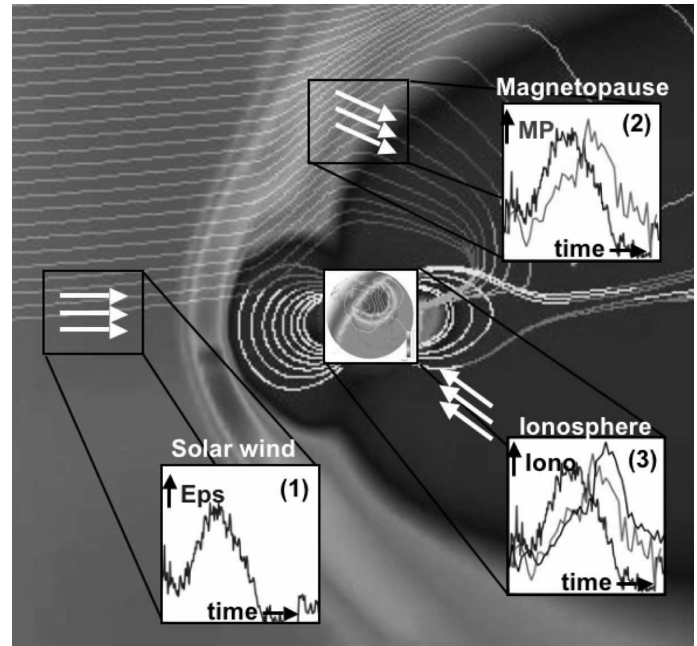
Fig. 3. Schematic of energy transfer process: (1) Epsilon in the solar wind; (2) Energy transferred through the magnetopause shows delay with respect to epsilon; (3) ionospheric energydissipation shows delay with respect to epsilon, but only a small delay with respect to energy input through magnetopause.

Fig. 2. in Run #: a-d) Instantaneous distributions of azimuthal magnetopause energy transfer at angles indicated by dashed vertical lines in panel (e). Grey areas indicate inward (towards magnetosphere) energy to sectors shown outside the outer circle. The sectors scale from 0 GW at the center to 800 GW at the outer circle. The IMF clock angle direction is indicated by a black arrow, while the black circles show the locations where reconnection is likely to occur [9]. e) Total transferred energy as function of clock angle (and time); the dashed line is $\sin^2(\theta/2)$ scaled to maximum and minimum of the energy transfer curve.

(2) The energy transfer through the magnetopause is best represented by a function proportional to $\sin^2(\theta/2)$, indicating that the energy transfer is better correlated with the solar wind electric field scaling as $\sin^2(\theta/2)$ than the ϵ parameter or Poynting flux scaling as $\sin^4(\theta/2)$.

These results would imply that the energy input after the substorm onset(when IMF turns northward or becomes less negative) is not accurately accounted for by using either ϵ or E_Y as a proxy for the energy input. The simulation results also hint for a stronger dependence of the energy transfer processes on the dynamic pressure than has been assumed before [12].

Recently, [8] criticize the dynamics in the global MHD simulations for being too directly driven by the solar wind and IMF driver. They assert that the "substorm in the magnetotail is hysteretic: Magnetic flux is added to the tail until the threshold of a still-undetermined instability in the tail is reached at which point unloading begins with the onset of a substorm". They suggest that the tail stability properties are asymmetric: An instability is triggered when a critical current density in the tail

is reached. Quenching of the instability occurs when the current density decreases to below another critical current density, smaller than what was required for the instability triggering. Using such formulation leads to a loading-unloading cycle in a driven current sheet even under continuous, steady driving. However, it is interesting to note that no such implementation of critical current density thresholds is needed at the global GUMICS-4 MHD simulation magnetopause to get the hysteretic behavior of the dayside reconnection line location and energy transfer efficiency.

The results presented here have possible implications in substorm dynamics and global energetics that follow. The substorm dynamic cycle can be described in the framework of a loading–unloading process: Growth-phase-associated enhanced energy input leads to a slow change of the magnetospheric state that at a later time allows for a global reconfiguration during the substorm expansion phase [3]. Because of this, and because of the time delays between the solar wind driver parameters such as ϵ and dissipation proxies such as AE, the energetics has been interpreted to also show signatures of loading and unloading. However, several studies indicate that this may not be the case: As demonstrated by [15], the energy input *during* the expansion phase, not prior to it, controls the substorm size as determined by ionospheric dissipation. Furthermore, [5] and [14] show respectively that only about a third of substorms show prior tail flux loading, and that there is no critical threshold of lobe magnetic flux that would lead to the substorm onset; these results also would indicate that the energy input prior to the onset is necessary for the configuration change to occur, but not to powering the substorm [13]. Lastly, the GUMICS-4 results

shown here and in [13] indicate that the time delays between the system input and output are nonexistent if one compares the actual energy input through the magnetopause to the ionospheric dissipation, while they do arise if one uses ϵ as a proxy for the energy input (see Fig. 3). Hence, if reconnection proves to be hysteretic in nature as the simulation suggests here and in [12], some of the time delays associated with the system input and output that have been interpreted as loading-unloading signatures, may already arise from processes taking place at the magnetopause.

Acknowledgements

References

1. Ahn, B.-H., S.-I. Akasofu, and Y. Kamide, The Joule heat production rate and the particle energy injection rate as a function of the geomagnetic indices AE and AL., *J. Geophys. Res., 88*, 6275, 1983.

2. Akasofu, S.-I., Energy coupling between the solar wind and the magnetosphere, *Space Sci. Rev., 28*, 121, 1981.

3. Baker, D. N., T. I. Pulkkinen, V. Angelopoulos, W. Baumjohann, and R. L. McPherron, The neutral line model of substorms: Past results and present view, *J. Geophys. Res., 101*, 12,975, 1996.

4. Cowley, S. W. H., Morelli, J. P., and Lockwood, M., Dependence of convective flows and particle precipitation in the high-latitude dayside ionosphere on the X and Y components of the interplanetary magnetic field, *J. Geophys. Res., 96*, 5557-5564, 1991.

5. Dmitreva, N. P., V. A. Sergeev, and M. A. Shukhtina, Average characteristics of the midtail plasma sheet in different dynamic regimes of the magnetosphere, *Ann. Geophys., 22*, 2107, SRef-ID: 1432-0576/ag/2004-22-2107, 2004.

6. Dungey, J. R., Interplanetary magnetic field and the auroral zones, *Phys. Rev. Lett., 6*, 47, 1961.

7. Janhunen, P., GUMICS-3: A global ionosphere-magnetosphere coupling simulation with high ionospheric resolution, in *Proceedings of Environmental Modelling for Space-based Applications*, ESA-SP 392, p. 205, 1996.

8. Klimas, A. J., V. M. Uritsky, D. Vassiliadis, and D. N. Baker, A mechanism for the loading-unloading substorm cycle missing in MHD global magnetospheric simulation models, *Geophys. Res. Lett., 32* (14), L14108, doi:10.1029/2005GL022916, 2005.

9. Laitinen, T. V, Janhunen, P., Pulkkinen, T. I., Palmroth, M., and Koskinen, H. E. J., On the characterization of magnetic reconnection in global MHD simulations, submitted to *Ann. Geophys.*, 2006.

10. Palmroth, M., T. I. Pulkkinen, P. Janhunen, C.-C. Wu, Stormtime energy transfer in global MHD simulation, *J. Geophys. Res., 108(A1)*, 1048, doi: 101029/2002JA009446, 2003.

11. Palmroth, M., P. Janhunen, T. I. Pulkkinen, and H. E. J. Koskinen, Ionospheric energy input as a function of solar wind parameters: global MHD simulation results, *Ann. Geophys., 22*, 549, 2004.

12. Palmroth, M., P. Janhunen, and T. I. Pulkkinen, Hysteresis in the solar wind power input into the magnetosphere, *Geophys. Res. Lett., 33*, L03107, doi:10.1029/2005GL025188), 2006.

13. Pulkkinen, T. I., M. Palmroth, E. I. Tanskanen, P. Janhunen, H. E. J. Koskinen, and T. V. Laitinen, New interpretation of magnetospheric energy circulation, *Geophys. Res. Lett., 33*, L07101, doi:10.1029/2005GL025457, 2006.

14. Shukhtina, M. A., N. P.Dmitreva, N. G. Popova, V. A. Sergeev, A. G. Yahnin, and I. V. Despirak, Observational evidence of the loading-unloading substorm scheme, *Geophys. Res. Lett., 32*, L17107, doi:10.1029/2005GL023779, 2005.

15. Tanskanen, E. I., T. I. Pulkkinen, H. E. J. Koskinen, Substorm energy budget near solar minimum and maximum: 1997 and 1999 compared, *J. Geophys. Res., 107*, A6, 10.1029/2001JA900153, 2002.